

Original Article

The effect of miR-27a on the proliferation, apoptosis, and chemosensitivity of non-small-cell lung cancer cells by targeting MCPH1

Yuxia Wu^{1*}, Rui Zhang^{2*}, Xiucheng Wang³, Mao Mao⁴, Penglong Li⁵

¹Department of Respiratory Medicine, Heze Municipal Hospital, Heze, Shandong Province, China; ²Department of Thoracic Surgery, Dezhou Second People's Hospital, Dezhou, Shandong Province, China; ³Department of Cardiothoracic Surgery, Zhucheng People's Hospital, Zhucheng, Shandong Province, China; ⁴Department of Oncology, Zibo City Traditional Chinese Medicine Hospital, Zibo, Shandong Province, China; ⁵Department of Oncology, Laiyang Central Hospital, Yantai, Shandong Province, China. *Equal contributors and co-first authors.

Received August 12, 2020; Accepted September 16, 2020; Epub December 15, 2020; Published December 30, 2020

Abstract: Objective: We aimed to investigate the effect of miR-27a on the proliferation, apoptosis, and chemosensitivity of non-small-cell lung cancer (NSCLC) cells by targeting microcephalin 1 (MCPH1). Methods: The targeting relationship between miR-27a and MCPH1 was first verified using a dual-luciferase reporter assay. The cell line A549 was chosen for the experiments as it has a higher miR-27a expression level than the other three NSCLC cell lines, H1355, H460, and H520. The proliferation ability of the NSCLC cells and the IC₅₀ values of doxorubicin and cisplatin for NSCLC cells were measured using MTT assays. The invasion ability of NSCLC cells was measured using a Transwell assay. The migration ability of NSCLC cells was measured using a wound healing assay. The cell cycle and cellular apoptosis rates were examined using flow cytometry. The mRNA and protein expression levels of MCPH1, PCNA, cyclin E1, Bcl-2, Bax, and caspase-3 were measured using qRT-PCR and western blot. Results: We found that miR-27a is highly expressed in NSCLC cells and can regulate MCPH1 expression. Moreover, silencing miR-27a can inhibit the proliferation, invasion, and migration of NSCLC cells, reduce the IC₅₀ values of doxorubicin and cisplatin, and promote NSCLC cell apoptosis. However, these effects of silencing miR-27a can be reversed by silencing MCPH1. Conclusion: miR-27a silencing can up-regulate MCPH1 expression, thereby inhibiting cell proliferation, invasion, and migration, inducing cellular apoptosis, and increasing the chemosensitivity of NSCLC cells.

Keywords: MicroRNAs, non-small cell lung cancer, cell proliferation, apoptosis, chemosensitivity, microcephalin 1

Introduction

Lung cancer is one of the most common cancers worldwide, and its morbidity and mortality have been rising rapidly over the past few decades [1]. Non-small-cell lung cancer (NSCLC) accounts for 80 to 85% of all lung cancers. It has been reported that there are about 500,000 new cases of NSCLC each year globally, and over half of the patients are aged over 65 years. Thus, NSCLC can be regarded as an aging-associated disease [2, 3]. There are many risk factors for NSCLC including smoking, a family history of lung cancer, environmental pollution, occupational exposure to cancer-causing agents, and an inappropriate diet [4]. According to some studies, around 75% of

patients are already at the middle to late stages when diagnosed with NSCLC and have a low five-year survival rate [5]. Due to the aging population in China, it is essential to find a feasible and effective way of treating this disease.

Some recent studies have reported that microcephalin 1 (MCPH1) may be a novel tumor suppressor gene, and its overexpression can induce the apoptosis of lung adenocarcinoma cells [6]. MCPH1, also known as BRIT1, was first discovered during the screening of the repressor of human telomerase reverse transcriptase. MCPH1 is located on chromosome 8p23.1, where various cancers including breast and ovarian cancer frequently show a loss of heterozygosity [7, 8]. The MCPH1 molecule contains

The effect of miR-27a on NSCLC cells by targeting MCPH1

BRCT (the carboxyl-terminus of BRCA1) domains related to phosphopeptide-binding sites. The BRCT domain widely exists in BRCA1, MDC1, and 53BP1 proteins, and these proteins are involved in the DNA damage response, DNA repair, and tumor suppression [9, 10]. Researchers have found that MCPH1 plays a vital role in the DNA damage-response pathway. Since DNA damage response is a key factor in the protection against early-stage cancer in the human body, we speculated that MCPH1 may have a great impact on tumor occurrence and development [11].

Previous studies have demonstrated that microRNAs (miRNAs) can markedly affect the proliferation, apoptosis, and chemosensitivity of NSCLC cells [12]. Zhang et al. reported an overexpression of miR-224 in liver cancer cells and concluded that miR-224 may be a key marker for liver cancer [13]. miRNA malfunction is associated with tumor occurrence, and miR-27a, as an oncogene, is overly expressed in cancers including breast cancer, ovarian cancer, gastric cancer, and colon cancer [14, 15]. The mechanism of miR-27a in tumor pathogenesis is complicated, and several downstream targets of this miRNA have been identified. In the present study, we investigated the effects of miR-27a and its target gene MCPH1 on the proliferation, apoptosis, and chemosensitivity of NSCLC cells, in an effort to find some new approaches to the clinical treatment of NSCLC.

Materials and methods

Cell culture

The normal human bronchial epithelial cell line 16HBE (ATCC, USA) and four NSCLC cell lines, A549, H1355, H460, and H520, were chosen and cultured in RPMI 1640 medium (Gibco, USA) containing 10% fetal bovine serum (Gibco, USA), 50 U/mL penicillin (Gibco, USA), and 100 µg/mL streptomycin (Gibco, USA) at 37°C with 5% CO₂ (incubator: Thermo3111, Jinan Beisheng, China). The medium was changed every two days and the cells were sub-cultured every 3-4 days.

Preparation of the liposome complexes

The transfection was performed using Lipofectamine 2000 (Invitrogen, USA). The miR-27a

inhibitor, miR-27a inhibitor NC, miR-27a mimics, miR-27a mimics NC, and si-MCPH1 (all 50 nmol/L, Vigenebio, USA) were centrifuged, mixed with 170 µL of phosphate-buffered saline (PBS, Thermo Fisher Scientific, USA), respectively, and then left to stand for 5 min. Next, 30 µL of Lipofectamine 2000 (Thermo Fisher Scientific, USA) was added to the samples followed by gentle agitation and incubation at room temperature for 20 min to create liposome complexes.

Grouping and transfection

The NSCLC cell line A549 in the logarithmic growth phase was seeded in 6-well plates at a density of 1×10^5 cells/well with six replicates for each group. Serum-free RPMI 1640 medium without penicillin-streptomycin were used 24 h before the transfection. The cells were divided into the following five groups: the blank group (untreated), the NC group (transfected with a negative control), the miR-27a inhibitor group (transfected with a miR-27a inhibitor), the si-MCPH1 group (transfected with si-MCPH1), and the miR-27a inhibitor + si-MCPH1 group (transfected with a miR-27a inhibitor and si-MCPH1). The transfection was conducted according to the Lipofectamine 2000 manufacturer's instructions. After 6 h of transfection, the medium was replaced with RPMI 1640 containing 10% fetal bovine serum (Gibco, USA).

Dual-luciferase reporter (DLR) assay

The targeting relationship between miR-27a and MCPH1 was analyzed through a bioinformatics website and verified using a DLR assay. The 3'UTR fragments of MCPH1 were amplified using PCR, and the PCR products were inserted into the multiple cloning sites located in the downstream of the luciferase gene in the pmirGLO (E1330, Promega, USA) for creating Wt-MCPH1. Meanwhile, the miR-27a binding site on MCPH1 predicted by the bioinformatics website was mutated, and the 3'UTR fragments of the mutant MCPH1 were amplified and cloned into the pmirGLO for creating Mut-MCPH1. The generation of Wt-MCPH1 and Mut-MCPH1 was performed by Huayueyang Biotechnology, Beijing, China. The miR-27a mimics and miR-27a mimics NC were co-transfected with DLR vectors, respectively, into 293T cells for measuring the luciferase activity.

The effect of miR-27a on NSCLC cells by targeting MCPH1

Table 1. qRT-PCR primer sequences

	Primer sequence
miR-27a	Forward: 5'-GATCTGCAGGGGTTAGCTTGGGGACCTGAAC-3' Reverse: 5'-GATCATATGAGAGTGACATACTGATGCCTAC-3'
MCPH1	Forward: 5'-GTGCCTATCTGTTGTATGACTG-3' Reverse: 5'-ATGTTAGACTGAGTAGGTGGCT-3'
PCNA	Forward: 5'-CTTATCTTCGCTAGGGGC-3' Reverse: 5'-ATGGACTGACTCGTCGTC-3'
Cyclin E1	Forward: 5'-CACCGGTAGAGTACTGAGCTC-3' Reverse: 5'-ACGAGTCCATTCGTCACGTGA-3'
Bcl-2	Forward: 5'-TATAAGCTGTCGAGAGGGG-3' Reverse: 5'-TGACGCTCTCCACACACATG-3'
Bax	Forward: 5'-TGCCAGCAAAGTGGTGTCA-3' Reverse: 5'-GCACTCCCGCCCAAAGATG-3'
Caspase-3	Forward: 5'-ATGGAGAACACTGAAAACCTCAG-3' Reverse: 5'-ATGGAGAACACTGAAAACCTCAG-3'
GAPDH	Forward: 5'-GGGCTGCTTTAACTCTGGT-3' Reverse: 5'-GCAGGTTTTTCTAGACGG-3'

Note: MCPH1, microcephalin 1; GAPDH: glyceraldehyde-3-phosphate dehydrogenase.

qRT-PCR

After 48 h of transfection, the total RNA was extracted from the cells in each group using TRIzol reagent (Invitrogen, USA). The RNAs were reverse transcribed into cDNAs using the PrimeScript™ RT kit (Takara, RRO47A, Beijing Think-far Technology Co., Ltd., China). A SYBR® Premix Ex Taq™ II kit (Xingzhi Biological Technology Co., Ltd., China) was used in the quantitative fluorescence PCR. The components of the reaction mixture were added in the following order: 25 µL of SYBR® Premix Ex Taq™ II (2×), 2 µL of forward PCR primer, 2 µL of reverse PCR primer, 1 µL of ROX reference dye (50×), 4 µL of DNA template, and 16 µL of double-distilled water. qRT-PCR (PCR device: ABI 7900HT) was performed according to the two-step protocol with the following parameters: 95°C for 30 s (pre-denaturation), and 40 cycles of 95°C for 5 s (denaturation), 58°C for 30 s (annealing), and 72°C for 15 s (extension). The relative expression levels of the target genes were calculated using the $2^{-\Delta\Delta Ct}$ method ($\Delta Ct = Ct_{\text{target gene}} - Ct_{\text{GAPDH}}$, $\Delta\Delta Ct = \Delta Ct_{\text{the study group}} - \Delta Ct_{\text{the control group}}$). GAPDH was used as the internal control, and the primers are listed in **Table 1**. The experiment was repeated three times.

Western blot

After 48 h of transfection, the cells were digested and collected, and the total protein was iso-

lated using RIPA (R0010, Solarbio) containing PMSF. The protein concentration was measured using a BCA kit (Thermo Fisher Scientific, USA) and adjusted with deionized water. The samples were then mixed with a loading buffer and heated in boiling water for 10 min. Next, 20 µg of protein samples were separated using 12% SDS-PAGE at 80 V for 2 h. The proteins were then transferred to a polyvinylidene fluoride (PVDF) membrane (ISEQ00010, Millipore, USA) using wet transfer at 110 V for 2 h. The PVDF membrane was blocked with 5% skim milk at 4°C for 2 h and then washed in Tris-buffered saline tween (TBST) followed by incubation with antibodies of rabbit anti-human MCPH1 (ab176524, 1:2,000, Abcam, UK), anti-PCNA (ab152112, 1:1,000, Abcam, UK), anti-cyclin E1 (ab71535, 1:2,000, Abcam, UK), anti-Bax (ab32503, 1:1,000, Abcam, UK), anti-Bcl-2 (ab32124, 1:1,000, Abcam, UK), anti-caspase-3 (ab197202, 1:1,000, Abcam, UK), and anti-GAPDH (ab8226, 1:2,000, Abcam, UK) at 4°C overnight. Next, the membrane was washed in TBST three times (10 min per wash) and incubated with horseradish peroxidase-conjugated goat anti-rabbit IgG antibody (Beijing, ZSbio, 1:5,000). Subsequently, the samples were washed in TBST and placed on a clean glass plate. Equal volumes of solutions A and B from an ECL kit (BB-3501, Amersham, UK) were mixed in the dark and added onto the membrane. The images were visualized using a

The effect of miR-27a on NSCLC cells by targeting MCPH1

gel-imaging system, photographed with a Bio-Rad imaging analyzer (BIO-RAD, USA), and analyzed using Image J software. The relative protein level was calculated as the grayscale value of the protein band/the grayscale value of GAPDH protein band. The experiment was repeated three times.

Cell proliferation ability and half-maximal inhibitory concentration (IC₅₀) measured by MTT assay

After 48 h of transfection, the cells were collected and counted. The cells were seeded in 96-well plates with six replicates for each group (100 μ L of $3\text{-}6 \times 10^3$ cells per well). At 24, 48, and 72 h, 20 μ L 5 mg/mL MTT solution (Gibco, USA) was dispensed into each well for a 4 h incubation in the dark. Subsequently, 100 μ L of DMSO was added to each well followed by 10 min agitation for dissolving. The optical density (OD) value at 490 nm was measured with a microplate reader (NYW-96M, Beijing Nuoyawei, China). Cell viability curves were plotted with time on the x-axis and the OD value on the y-axis. The assay was repeated three times.

To measure the IC₅₀, the cells were seeded into the 96-well plates in the same way as described above. The cells untreated with cisplatin and doxorubicin were used as controls. Cisplatin with concentrations of 0.01, 0.1, 1, 10, and 100 μ g/mL and doxorubicin with concentrations of 0.01, 0.05, 0.25, 1.25, 5, and 25 μ g/mL were added, correspondingly, into each group (each group had 6 replicates). After 48 h of culture, 20 μ L 5 mg/mL MTT (Gibco, USA) was dispensed into the wells for 4 h of culture in the dark. Next, 100 μ L of DMSO was added to each well followed by agitation for 10 min. The OD value at 490 nm was measured with a microplate reader (NYW-96M, Beijing Nuoyawei, China), and the formula for the cell growth inhibitory rate (GIR) was as follows:
$$\text{GIR} = \frac{(\text{OD}_{\text{the control group}} - \text{OD}_{\text{the study group}}) / \text{OD}_{\text{the control group}}}{1} \times 100\%$$
The concentration-effect curve was plotted using SPSS software with log (concentration) on the x-axis and GIR on the y-axis for IC₅₀ value calculation. The experiment was repeated three times to calculate the mean and the standard deviation.

The cell cycle and apoptosis quantified using flow cytometry

After 48 h of transfection, the cells were harvested to determine the cell cycle distribution.

The cells were washed in PBS three times and centrifuged at $200 \times g$ for 5 min. After we discarded the supernatant, we adjusted the cell density to 1×10^6 /mL with PBS, and then we fixed the cells with 1 mL 75% pre-cooled ethanol at 4°C for 1 h. Next, the cells were centrifuged at $200 \times g$ for 5 min followed by two rinses in PBS. RNase A (100 μ L, Thermo Fisher Scientific, USA) was added, and the samples were placed in a 37°C water bath in the dark for 30 min followed by staining with 400 μ L of propidium iodide (PI, Sigma, USA) at 4°C in the dark for 30 min. The cell cycle was examined with a flow cytometer (Beckman Coulter, USA) using red fluorescence at an excitation wavelength of 488 nm. The experiment was repeated three times.

After 48 h of transfection, the cells were digested with EDTA-free pancreatin (Thermo Fisher Scientific, USA) and placed in flow cytometry tubes for measuring the cell apoptosis. After centrifugation at $12,000 \times g$ for 30 min, the supernatant was discarded, and the cells were washed in cold PBS three times. The samples were centrifuged again at $12,000 \times g$ for 15 min before supernatant was removed. According to the manufacturer's instructions of the Annexin-V-fluorescein isothiocyanate (FITC) apoptosis detection kit (Sigma, USA), Annexin-V-FITC/PI dye was prepared using HEPES buffer, Annexin-V-FITC, and PI (50:1:2). The cells were mixed with 100 μ L of dye and incubated at room temperature for 15 min. Subsequently, the samples were treated with 1 mL of HEPES buffer (Thermo Fisher Scientific, USA) followed by agitation and mixing. The cell apoptosis was examined at an excitation wavelength of 488 nm with a flow cytometer. The cellular apoptosis rate was calculated as apoptotic cell count/total cell count * 100%. The experiment was repeated three times.

The cell migration in each group was measured using a wound healing assay

After 48 h of transfection, the cells were seeded in 6-well plates at a density of 5×10^5 cells/well. When the cells reached 90% confluence, a scratch was gently made across the central axis line of the well with a sterile pipette tip, and each wound width remained the same. A serum-free medium was added for the culturing, and the cells were photographed at 0 and 24 h after being scratched. The cell migration distance was measured using Image-Pro Plus Analysis software (Media Cybernetics, USA).

The effect of miR-27a on NSCLC cells by targeting MCPH1

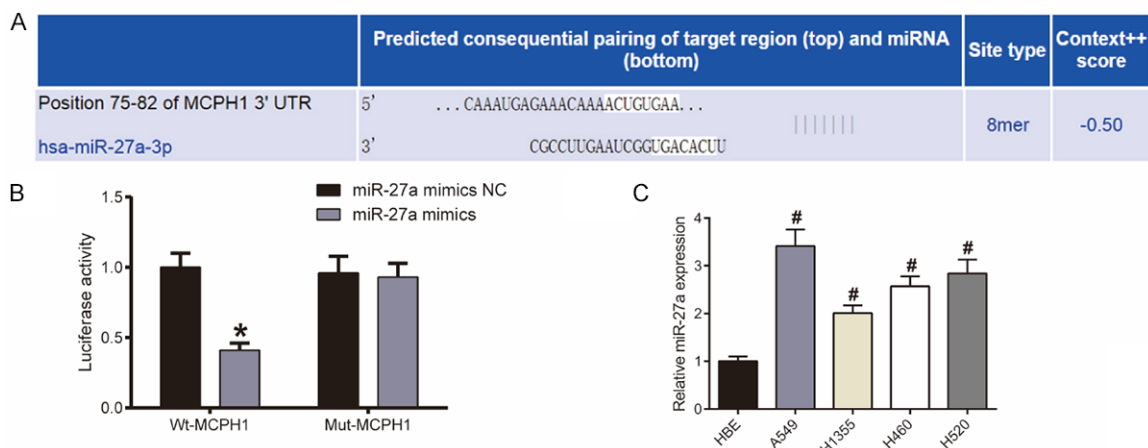


Figure 1. miR-27a can negatively regulate the MCPH1 gene. A. The sequence of the 3'-UTR region for the pairing of miR-27a with MCPH1; B. Luciferase activity determined using a dual-luciferase reporter assay; C. The expression levels of miR-27a in 16HBE and NSCLC cells A549, H1355, H460, and H520. *P < 0.05 vs the miR-27a mimics NC group, #P < 0.05 vs 16HBE. MCPH1: microcephalin 1; NSCLC: non-small-cell lung cancer.

Migration rate = (wound width at 0 h after scratch - wound width at 24 h after scratch)/wound width at 0 h after scratch. Multiple fields were selected randomly to photograph. Each group had three replicates, and the experiment was repeated three times.

The cell invasion in each group was measured using Transwell assays

Transwell chambers (Shanghai Jrdun Biotechnology, China) were placed in 24-well plates, and the upper side of the Transwell insert was pre-coated with Matrigel (1:8, Shanghai Qcbio, China) followed by drying at room temperature. The cells in each group were digested and washed in PBS twice. The cell density was 1×10^5 /mL after resuspension with medium. The cell suspension (200 μ L) was added into the Transwell upper chamber and 600 μ L of RPMI 1640 medium was added into the lower chamber. After 24 h, the cells at the inner side of the upper chamber were scraped off using a cotton swab and were fixed with 4% paraformaldehyde (Beijing Leagene Biotechnology, China) at room temperature for 10 min before being washed twice in PBS. Subsequently, the cells were stained with 0.5% crystal violet (Beijing Solarbio, China) for 15 min and washed in PBS three times. Under an inverted microscope, five fields from each group were randomly selected for observation (200X). The cells that had invaded through the membranes were counted and photographed.

Statistical analysis

SPSS 21.0 was applied for the statistical analysis. The measurement data are expressed as the mean \pm standard deviation ($x \pm sd$). The comparisons between multiple groups were conducted using one-way analyses of variance. The pairwise comparisons of the mean values in multiple groups were conducted using Tukey's post-hoc tests. P < 0.05 was considered to indicate a statistically significant difference.

Results

miR-27a is highly expressed in NSCLC cells

The bioinformatics website (<http://www.microrna.org/microrna/home.do>) predicted the existence of the miR-27a binding site on MCPH1 (**Figure 1A**). Moreover, the results of the DLR assay showed that, compared with the cells transfected with the miR-27a mimics NC, the cells co-transfected with the miR-27a mimics and Wt-MCPH1 had lowered the luciferase activity (P < 0.05) and the cells co-transfected with the miR-27a mimics and Mut-MCPH1 had similar luciferase activity (P > 0.05, **Figure 1B**). These results indicate that miR-27a can negatively regulate the MCPH1 gene.

Meanwhile, qRT-PCR was conducted to determine the expression levels of miR-27a in the normal human bronchial epithelial cell line

The effect of miR-27a on NSCLC cells by targeting MCPH1

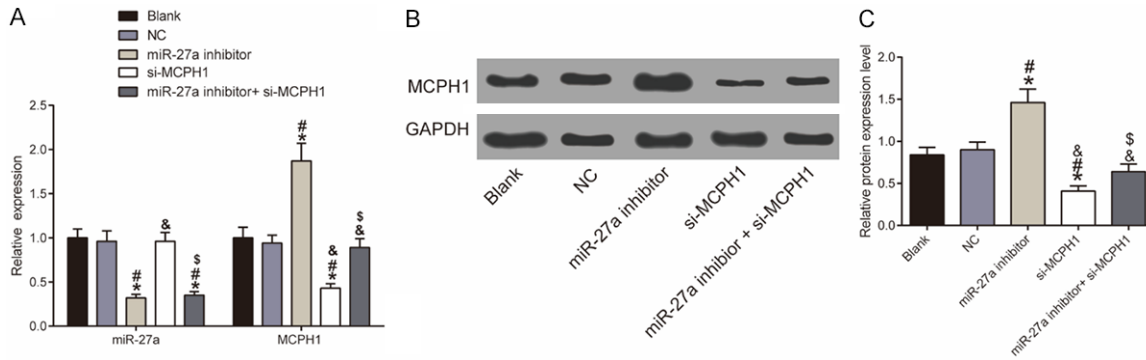


Figure 2. miR-27a and MCPH1 mRNA expression levels measured using qRT-PCR and the MCPH1 protein expression level measured using western blot. A. Histogram of the qRT-PCR results; B. Western blot bands; C. Histogram of the western blot results. * $P < 0.05$ vs the blank group; # $P < 0.05$ vs the NC group; [#] $P < 0.05$ vs the miR-27a inhibitor group; [§] $P < 0.05$ vs the si-MCPH1 group. MCPH1: microcephalin 1.

16HBE and in the NSCLC cell lines A549, H1355, H460, and H520. The results showed that, compared with 16HBE, the four cancer cell lines had much higher levels of miR-27a, and the expression level of this miRNA was highest in A549 (all $P < 0.05$). Thus, the A549 cell line was chosen for the subsequent experiments (**Figure 1C**).

The expression levels of miR-27a and MCPH1 in each group

In order to verify the transfection results, we performed qRT-PCR to measure the mRNA expression levels of miR-27a and MCPH1 in each group. The results showed no differences in the gene expression levels between the blank and NC groups (both $P > 0.05$). Compared with the blank group, the miR-27a expression levels in the miR-27a inhibitor and miR-27a inhibitor + si-MCPH1 groups as well as the MCPH1 mRNA expression level in the si-MCPH1 group were much lower (all $P < 0.05$). See **Figure 2A**.

Also, the western blot results showed that the MCPH1 protein expression levels in the blank and miR-27a inhibitor + si-MCPH1 groups were not significantly different from their levels in the NC group, (both $P > 0.05$), but the miR-27a inhibitor group had higher MCPH1 protein expression levels and the si-MCPH1 group had lower MCPH1 protein expression levels compared with the NC group (both $P < 0.05$). See **Figure 2B and 2C**.

The cell proliferation abilities and IC_{50} values of doxorubicin and cisplatin measured using MTT assays

The results of the MTT assays showed that the blank and miR-27a inhibitor + si-MCPH1 groups had similar cell proliferation abilities compared to the NC group ($P > 0.05$). At 48 and 72 h, the cell proliferation ability was lower in the miR-27a inhibitor group and was higher in the si-MCPH1 group compared with the NC group (all $P < 0.05$). Moreover, the cell proliferation ability was greater in the miR-27a inhibitor + si-MCPH1 group than it was in the miR-27a inhibitor group at 48 and 72 h (both $P < 0.05$). The findings suggest that silencing miR-27a can inhibit the proliferation of NSCLC cell A549, but this effect of silencing miR-27a on A549 can be reversed by silencing MCPH1. See **Figure 3A**.

The results of the MTT assay indicated that the IC_{50} values of doxorubicin and cisplatin for the NSCLC cells in the blank and miR-27a inhibitor + si-MCPH1 groups were not different from the IC_{50} values of doxorubicin and cisplatin for the NSCLC cells in the NC group (all $P > 0.05$), but the IC_{50} values were lower in the miR-27a inhibitor group and higher in the si-MCPH1 group compared with the NC group (all $P < 0.05$). The doxorubicin and cisplatin IC_{50} values in the miR-27a inhibitor + si-MCPH1 group were higher than they were in the miR-27a inhibitor group and lower than they were in the si-MCPH1 group (all $P < 0.05$). The results indicate that silencing miR-27a can reduce the resistance of NSCLC

The effect of miR-27a on NSCLC cells by targeting MCPH1

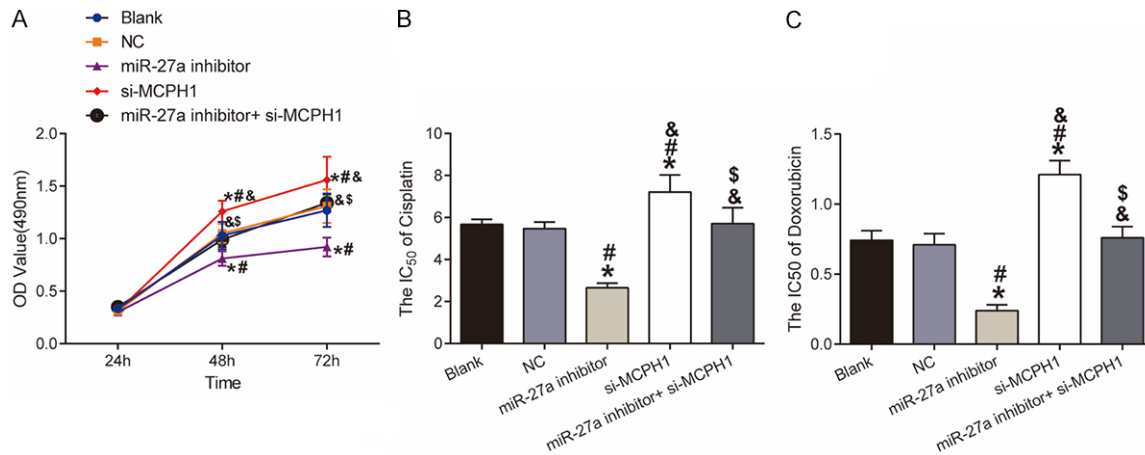


Figure 3. The cell proliferation abilities and IC₅₀ values of doxorubicin and cisplatin for the NSCLC cells measured using MTT assays. A. Cell proliferation ability measured using an MTT assay; B. The IC₅₀ value of cisplatin in each group; C. The IC₅₀ value of doxorubicin in each group. *P < 0.05 vs the blank group; #P < 0.05 vs the NC group; &P < 0.05 vs the miR-27a inhibitor group; \$P < 0.05 vs the si-MCPH1 group. IC₅₀: half maximal inhibitory concentration; MCPH1: microcephalin 1; OD: optical density; NSCLC: non-small-cell lung cancer.

cell line A549 to doxorubicin and cisplatin. See **Figure 3B** and **3C**.

Cell cycle measured by flow cytometry

A flow cytometry test showed that, compared with the NC group, the miR-27a inhibitor group had a higher proportion of A549 cells in the G1 phase and a lower proportion of cells in the S phase, but the si-MCPH1 had a lower proportion of G1 cells and a higher proportion of S cells (all P < 0.05). No differences were found among the blank, NC, or miR-27a inhibitor + si-MCPH1 groups in terms of cell cycle distribution (P > 0.05). The miR-27a inhibitor + si-MCPH1 group had a lower proportion of cells in the G1 phase and a higher proportion of cells in the S phase versus the miR-27a inhibitor group (both P < 0.05). The findings suggest that silencing miR-27a can hinder cell cycle progression and arrest the cells in the G1 phase in the A549 cell line. However, the effect of silencing miR-27a can be reversed using MCPH1 silencing. See **Figure 4**.

Cellular apoptosis measured by flow cytometry

Compared with the NC group, the miR-27a inhibitor group had a higher cellular apoptosis rate (P < 0.05), but the other groups had similar cellular apoptosis rates (all P > 0.05). The miR-27a inhibitor + si-MCPH1 group had a lower apoptosis rate than the miR-27a inhibitor group (P < 0.05). The results demonstrated that

silencing miR-27a can promote the apoptosis of NSCLC cell A549, whereas this effect of silencing miR-27a can be reversed by silencing MCPH1. See **Figure 5**.

Cell migration ability measured using wound healing assays

Compared with the NC group, the cell migration ability was lower in the miR-27a inhibitor group and higher in the si-MCPH1 group (both P < 0.05). Meanwhile, the cell migration ability in the miR-27a inhibitor + si-MCPH1 group was higher compared with the miR-27a inhibitor group and lower compared with the si-MCPH1 group (both P < 0.05). These results suggest that silencing miR-27a can suppress the migration ability of NSCLC cell A549, and silencing MCPH1 can promote the migration of A549. See **Figure 6**.

Cell invasion ability measured using Transwell assays

The blank and the miR-27a inhibitor + si-MCPH1 groups had similar amounts of invading cells compared with the NC group (both P > 0.05), but the amount of invading cells was lower in the miR-27a inhibitor group and higher in the si-MCPH1 group compared with the NC group (both P < 0.05). The miR-27a inhibitor + si-MCPH1 group had more invading cells than the miR-27a inhibitor group and fewer invading cells than the si-MCPH1 group (both P < 0.05).

The effect of miR-27a on NSCLC cells by targeting MCPH1

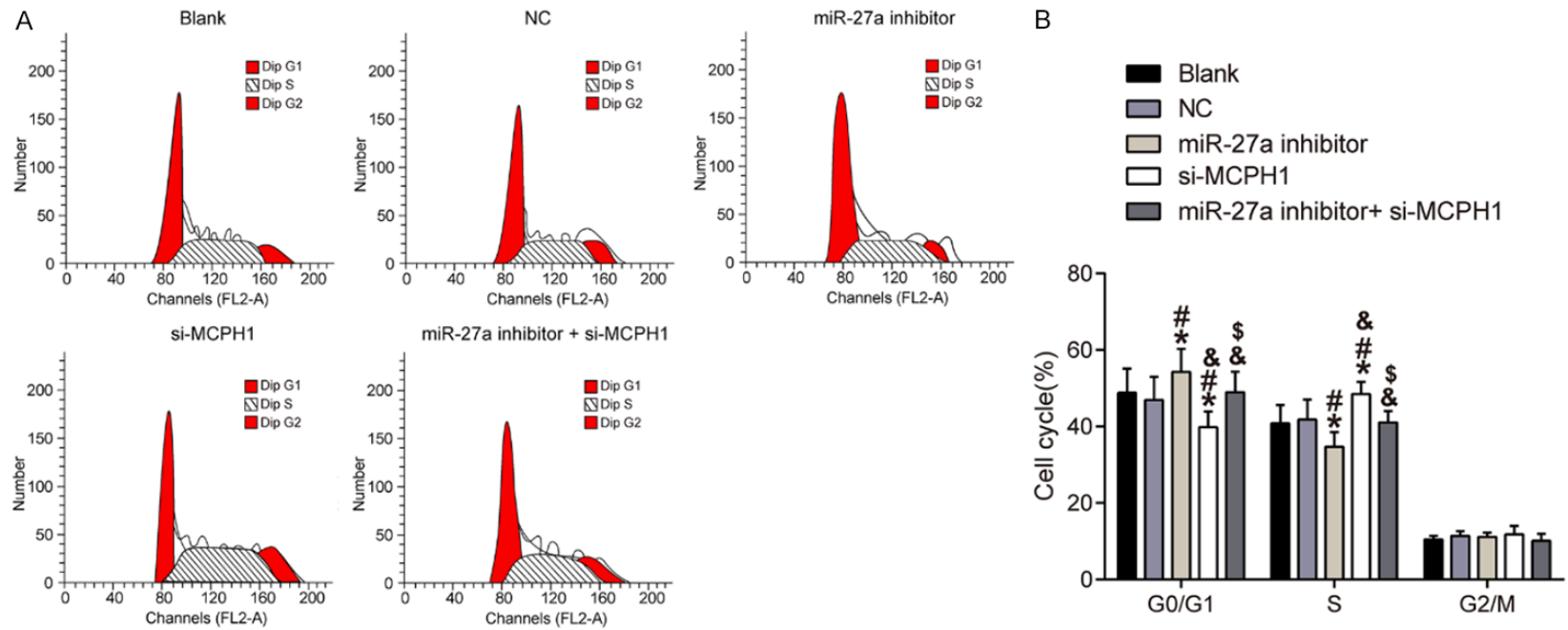


Figure 4. Flow cytometric analysis of the cell cycle in each group. A. The cell cycle distribution in each group; B. Histograms of the cell cycle in each group. *P < 0.05 vs the blank group; #P < 0.05 vs the NC group; &P < 0.05 vs miR-27a inhibitor group; \$P < 0.05 vs the si-MCPH1 group. MCPH1: microcephalin 1.

The effect of miR-27a on NSCLC cells by targeting MCPH1

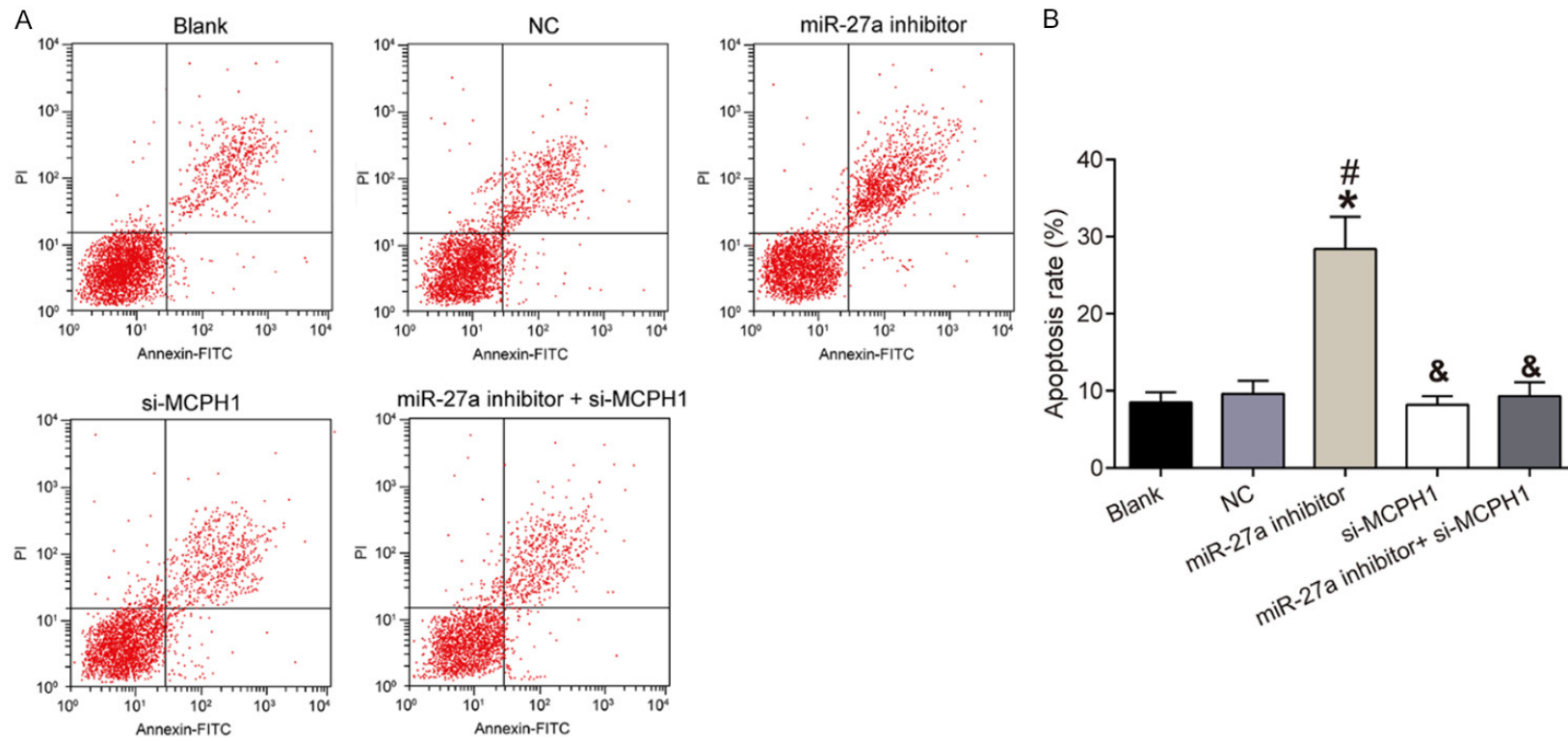


Figure 5. Flow cytometric analysis of the cell apoptosis in each group. A. The cell apoptosis in each group; B. A histogram of the cell apoptosis rate in each group. *P < 0.05 vs the blank group; #P < 0.05 vs the NC group; &P < 0.05 vs miR-27a inhibitor group. MCPH1: microcephalin 1; FITC: fluorescein isothiocyanate.

The effect of miR-27a on NSCLC cells by targeting MCPH1

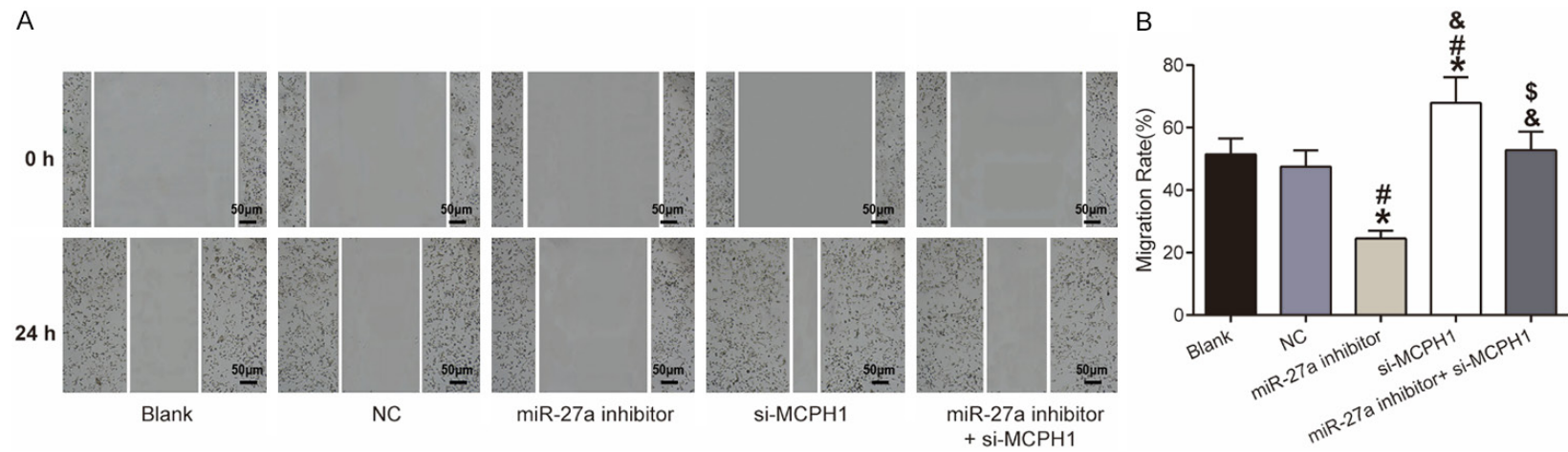


Figure 6. The cell migration ability in each group measured using wound healing assays. A. The wound in each group (cropped gel); B. A histogram of the cell migration rate in each group. *P < 0.05 vs the blank group; #P < 0.05 vs the NC group; &P < 0.05 vs miR-27a inhibitor group; \$P < 0.05 vs the si-MCPH1 group. MCPH1: microcephalin 1.

The effect of miR-27a on NSCLC cells by targeting MCPH1

The results indicate that silencing miR-27a can suppress the invasion ability of NSCLC cell A549, whereas silencing MCPH1 can promote the invasion of A549. See **Figure 7**.

mRNA and protein expression levels of PCNA, cyclin E1, Bcl-2, Bax, and caspase-3 in each group

In order to investigate the effect of MCPH1 overexpression on the proliferation, apoptosis, and chemosensitivity of NSCLC cells by mediating the ATR signaling pathway, we measured the mRNA and protein expressions of PCNA, cyclin E1, Bcl-2, Bax, and caspase-3 using qRT-PCR and Western blot. The results, displayed in **Figure 8**, showed no differences in their mRNA and protein expression levels of PCNA, cyclin E1, Bcl-2, Bax, or caspase-3 among the blank, NC, and miR-27a inhibitor + si-MCPH1 groups (all $P > 0.05$). Compared with the NC group, the miR-27a inhibitor group had lower mRNA and protein expression levels of PCNA, cyclin E1, and Bcl-2 and higher mRNA and protein expression levels of Bax and caspase-3. In contrast, the si-MCPH1 group had higher mRNA and protein levels of PCNA, cyclin E1, and Bcl-2 and lower mRNA and protein levels of Bax and caspase-3 than the NC group (all $P < 0.05$). Compared with the miR-27a inhibitor group, the miR-27a inhibitor + si-MCPH1 group had higher mRNA and protein expression levels of PCNA, cyclin E1, and Bcl-2 and lower mRNA and protein expression levels of Bax and caspase-3 (all $P < 0.05$). These results indicate that silencing miR-27a can suppress the mRNA and protein expression levels of the proliferation-related factors, PCNA and cyclin E1, and the anti-apoptotic factor, Bcl-2, and promote the mRNA and protein expression levels of the pro-apoptotic factors, Bax and caspase-3, in NSCLC cell A549.

Discussion

According to some surveys, the morbidity of lung cancer increases with senescence, and the age of onset is now 5-10 years earlier than before. Currently, the therapies for treating lung cancer cannot achieve good results in elderly patients, as the elderly people have weakened metabolic and organ functions, many concomitant diseases, and a poor tolerance to chemotherapy. Since molecularly targeted therapy has become a breakthrough in the clinical

treatment of lung cancer in recent years, we aimed to investigate NSCLC from a molecular-level perspective in this study, in an effort to bring some new insights into the gene therapy for this disease.

We first found the pairing of miR-27a with MCPH1 using a bioinformatics website and verified their relationship by conducting a DLR assay. Previous studies have already revealed that miRNA can affect cancer cells via regulating target genes. For instance, miR-181a-5p can target Kras to suppress the proliferation and migration of NSCLC cells.

MCPH1 has become a popular research topic in recent years. Clinical trials have demonstrated that the aberrant expression of MCPH1 is closely related to the occurrence and development of tumors [15]. MCPH1, which can regulate the cell cycle and participate in various regulations of cellular functions, has a key role in the DNA damage response pathway, and DNA damage is considered a major cause of cancer [16, 17]. Previous studies reported a low expression level of MCPH1 in human lung cancer tissue and a high expression level in normal lung tissue and revealed that the high expression of MCPH1 can help to inhibit the proliferation and induce the apoptosis of human lung cancer cells [18]. Moreover, some in vitro studies have indicated that MCPH1 is an indispensable nucleobindin that can help other DNA damage response proteins gain access to the DNA lesions [19]. When DNA damage occurs, MCPH1 can maintain genome stability via the ATM/ATR signaling pathway [20, 21].

In our study, we found that silencing miR-27a can up-regulate MCPH1 expression, inhibit the proliferation, migration, and invasion, and increase the apoptosis rate in the NSCLC cell line A549; moreover, the pro-apoptotic effect of silencing miR-27a is reversed by silencing MCPH1. Also, we found that silencing miR-27a reduces the resistance of NSCLC cell line A549 to doxorubicin and cisplatin. Doxorubicin and cisplatin are common chemotherapeutic drugs for treating lung cancer. Doxorubicin can inhibit RNA and DNA synthesis and can kill tumor cells in different growth cycles, and cisplatin can suppress DNA replication and damage cancer cells' membrane structures [22, 23]. Furthermore, we found that miR-27a silencing

The effect of miR-27a on NSCLC cells by targeting MCPH1

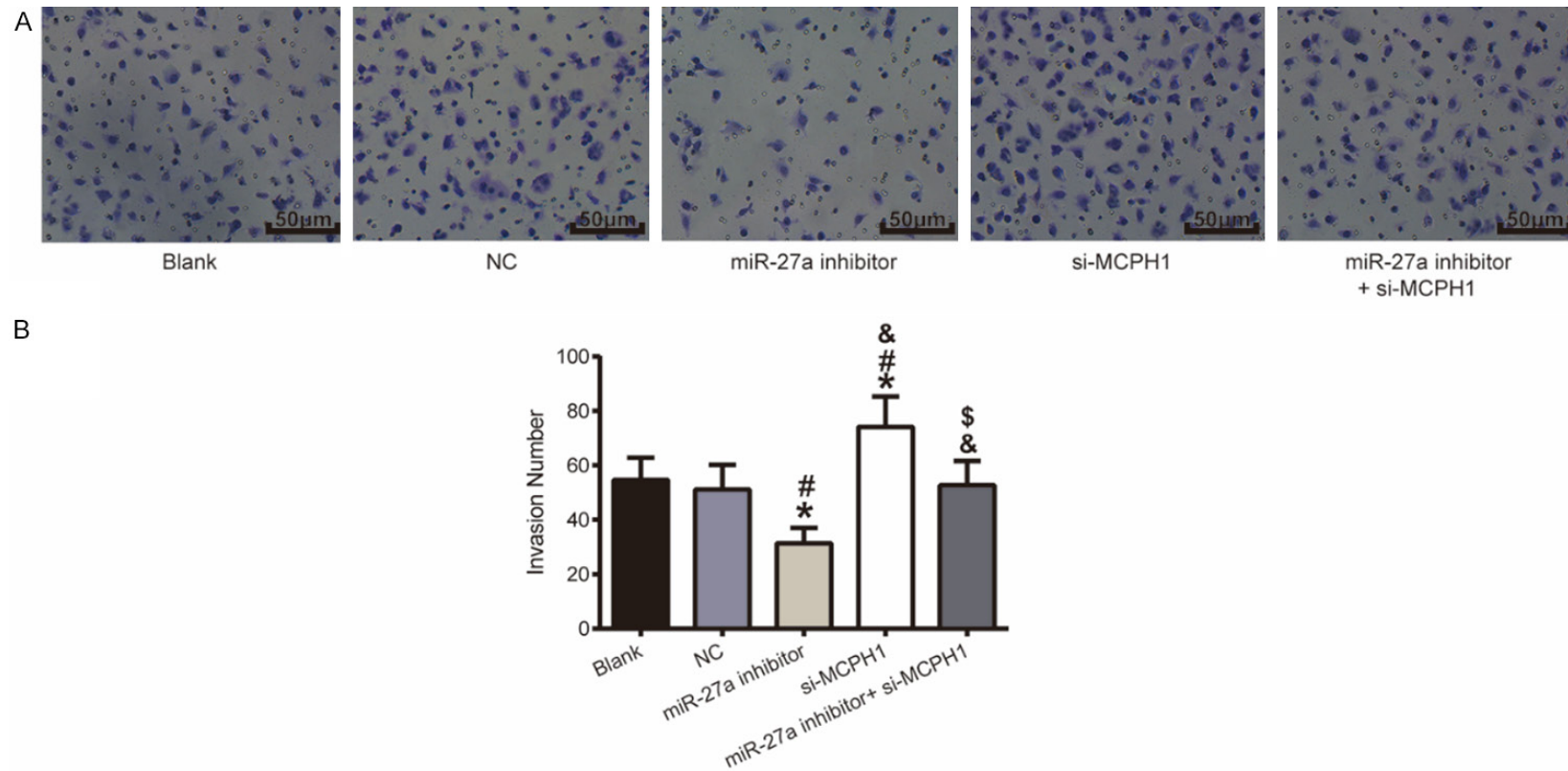


Figure 7. The cell invasion ability in each group measured using Transwell assays (200 \times). A. Images of the cell invasion in each group; B. The number of invasive cells in each group. * $P < 0.05$ vs the blank group; # $P < 0.05$ vs the NC group; & $P < 0.05$ vs miR-27a inhibitor group; \$ $P < 0.05$ vs the si-MCPH1 group. MCPH1: microcephalin 1.

The effect of miR-27a on NSCLC cells by targeting MCPH1

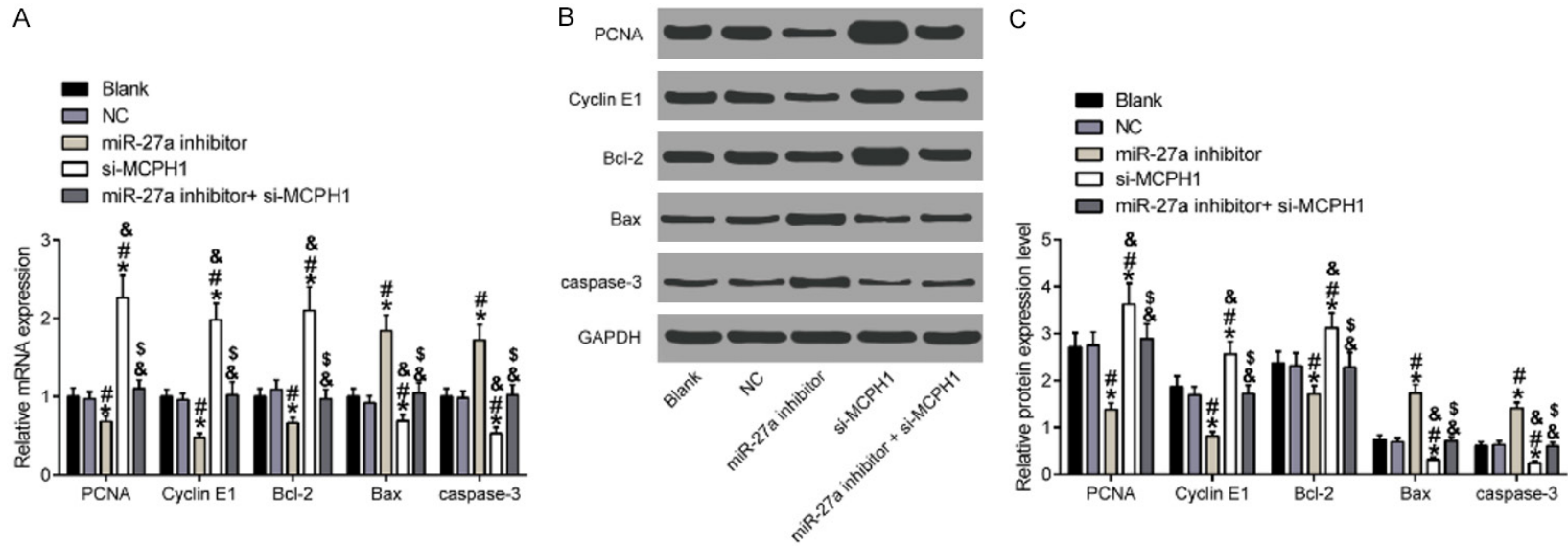


Figure 8. The mRNA and protein expressions of PCNA, cyclin E1, Bcl-2, Bax, and caspase-3 measured using qRT-PCR and Western blot. A. The mRNA expression levels of the genes in each group; B. Protein band image (cropped blot); C. The protein expression levels in each group. *P < 0.05 vs the blank group; #P < 0.05 vs the NC group; &P < 0.05 vs the miR-27a inhibitor group; \$P < 0.05 vs the si-MCPH1 group. MCPH1: microcephalin 1.

can inhibit the mRNA and protein expressions of PCNA, cyclin E1, and Bcl-2 and promote the mRNA and protein expressions of Bax in A549. PCNA and cyclin E1 participate in cell proliferation, but Bcl-2 and Bax are an anti-apoptotic factor and a pro-apoptotic factor, respectively [24, 25]. However, further investigations need to be conducted to elucidate the detailed mechanism by which MCPH1 induces cellular apoptosis.

In conclusion, silencing miR-27a can up-regulate MCPH1 expression, thereby inhibiting cell proliferation, invasion, and migration, inducing cellular apoptosis, and increasing the chemosensitivity of NSCLC cells. However, more studies need to be conducted to explore the signaling pathways miR-27a uses to regulate the MCPH1 expression in NSCLC cells.

Disclosure of conflict of interest

None.

Address correspondence to: Penglong Li, Department of Oncology, Laiyang Central Hospital, No. 111 Changshan Road, Yantai 265200, Shandong Province, China. Tel: +86-0535-7228239; E-mail: lipenglong98ly@163.com

References

- [1] Abbosh C, Birkbak NJ, Wilson GA, Jamal-Hanjani M, Constantin T, Salari R, Quesne JL, Moore DA, Veeriah S, Rosenthal R, Marafioti T, Kirkizlar E, Watkins TBK, McGranahan N, Ward S, Martinson L, Riley J, Fraioli F, Bakir MA, Grönroos E, Zambrana F, Endozo R, Bi WL, Fenessy FM, Sponer N, Johnson D, Laycock J, Shafi S, Czyzewska-Khan J, Rowan A, Chambers T, Matthews N, Turajlic S, Hiley C, Lee SM, Forster MD, Ahmad T, Falzon M, Borg E, Lawrence D, Hayward M, Kolvekar S, Panagiotopoulos N, Janes SM, Thakrar R, Ahmed A, Blackhall F, Summers Y, Hafez D, Naik A, Ganguly A, Kareht S, Shah P, Joseph L, Quinn AM, Crosbie PA, Naidu B, Middleton G, Langman G, Trotter S, Nicolson M, Remmen H, Kerr K, Chetty M, Gomersall L, Fennell DA, Nakas A, Rathinam S, Anand G, Khan S, Russell P, Ezhil V, Ismail B, Irvin-Sellers M, Prakash V, Lester JF, Kornaszewska M, Attanoos R, Adams H, Davies H, Oukrif D, Akarca AU, Hartley JA, Lowe HL, Lock S, Iles N, Bell H, Ngai Y, Elgar G, Szallasi Z, Schwarz RF, Herrero J, Stewart A, Quezada SA, Peggs KS, Loo PV, Dive C, Lin CJ, Rabinowitz M, Aerts HJWL, Hackshaw A, Shaw JA, Zimmermann BG and Swanton C. Phylogenetic ctDNA analysis depicts early-stage lung cancer evolution. *Nature* 2017; 545: 446-451.
- [2] Jamal-Hanjani M, Wilson GA, McGranahan N, Birkbak NJ, Watkins TBK, Veeriah S, Shafi S, Johnson DH, Mitter R, Rosenthal R, Salm M, Horswell S, Escudero M, Matthews N, Rowan A, Chambers T, Moore DA, Turajlic S, Xu H, Lee S, Forster MD, Ahmad T, Hiley CT, Abbosh C, Falzon M, Borg E, Marafioti T, Lawrence D, Hayward M, Kolvekar S, Panagiotopoulos N, Janes SM, Thakrar R, Ahmed A, Blackhall F, Summers Y, Shah R, Joseph L, Quinn AM, Crosbie PA, Naidu B, Middleton G, Langman G, Trotter S, Nicolson M, Remmen H, Kerr K, Chetty M, Gomersall L, Fennell DA, Nakas A, Rathinam S, Anand G, Khan S, Russell P, Ezhil V, Ismail B, Irvin-Sellers M, Prakash V, Lester JF, Kornaszewska M, Attanoos R, Adams H, Davies H, Dentro S, Taniere P, O'Sullivan B, Lowe HL, Hartley JA, Iles N, Bell H, Ngai Y, Shaw JA, Herrero J, Szallasi Z, Schwarz RF, Stewart A, Quezada SA, Quesne JL, Loo PV, Dive C, Hackshaw A and Swanton C. Tracking the evolution of non-small-cell lung cancer. *N Engl J Med* 2017; 376: 2109-2121.
- [3] Zhou FZ, Nie L, Feng DL, Guo SY and Luo RN. MicroRNA-379 acts as a tumor suppressor in non-small cell lung cancer by targeting the IG-F1R-mediated AKT and ERK pathways. *Oncol Rep* 2017; 38: 1857-1866.
- [4] Tang TT, Huan LT, Zhang SJ, Zhou H, Gu L, Chen XH and Zhang L. MicroRNA-212 functions as a tumor-suppressor in human non-small cell lung cancer by targeting SOX4. *Oncol Rep* 2017; 38: 2243-2250.
- [5] Carbone DP, Reck M, Paz-Ares L, Creelan B, Horn L, Steins M, Felip E, van den Heuvel MM, Ciuleanu T, Badin F, Ready N, Hiltermann TJN, Nair S, Juergens R, Peters S, Minenza E, Wrangle JM, Rodriguez-Abreu D, Borghaei H, Blumenschein GR Jr, Villaruz LC, Havel L, Krejci J, Jaime JC, Chang H, Geese WJ, Bhagavatheeswaran P, Chen AC and Socinski MA. First-line nivolumab in stage IV or recurrent non-small-cell lung cancer. *N Engl J Med* 2017; 376: 2415-2426.
- [6] Liu XQ, Zong W, Li TL, Wang YJ, Xu XZ, Zhou ZW and Wang ZQ. The E3 ubiquitin ligase APC/C (C) (dh1) degrades MCPH1 after MCPH1-betaTrCP2-Cdc25A-mediated mitotic entry to ensure neurogenesis. *EMBO J* 2017; 36: 3666-3681.
- [7] Duerinckx S, Meuwissen M, Perazzolo C, Desmyter L, Pirson I and Abramowicz M. Phenotypes in siblings with homozygous mutations of TRAPPC9 and/or MCPH1 support a bifunctional model of MCPH1. *Mol Genet Genomic Med* 2018; 6: 660-665.
- [8] Naseer MI, Rasool M, Muthaffar OY, Sabbagh AJ, Chaudhary AG and Al-Qahtani MH. A novel

The effect of miR-27a on NSCLC cells by targeting MCPH1

- homozygous frameshift variant in the MCPH1 gene causes primary microcephaly in a consanguineous Saudi family. *Genes Genomics* 2017; 39: 1317-1323.
- [9] Wood JL, Singh N, Mer G and Chen JJ. MCPH1 functions in an H2AX-dependent but MDC1-independent pathway in response to DNA damage. *J Biol Chem* 2007; 282: 35416-35423.
- [10] Liang Y, Gao H, Lin SY, Peng G, Huang XX, Zhang PM, Goss JA, Brunicardi FC, Multani AS, Chang S and Li KY. BRIT1/MCPH1 is essential for mitotic and meiotic recombination DNA repair and maintaining genomic stability in mice. *PLoS Genet* 2010; 6: e1000826.
- [11] Wu XB, Liu W, Liu XL, Ai Q and Yu JL. Overexpression of MCPH1 inhibits the migration and invasion of lung cancer cells. *Oncotargets Ther* 2018; 11: 3111-3117.
- [12] McMullen S, Hess LM, Kim ES, Levy B, Mohamed M, Waterhouse D, Wozniak A, Goring S, Müller K, Muehlenbein C, Aggarwal H, Zhu YJ, Oton AB, Ersek JL and Winfree KB. Treatment decisions for advanced non-squamous non-small cell lung cancer: patient and physician perspectives on maintenance therapy. *Patient* 2019; 12: 223-233.
- [13] Zhang HY, Lu JB, Yang W and Chen KB. Expression of miR-224 and miR-135a in non-small cell lung cancer and the relation with clinical pathology. *J Mod Oncol* 2012; 20: 2057-2059.
- [14] Zhang HW, Li MB, Han Y, Hong L, Gong TQ, Sun L and Zheng XS. Down-regulation of miR-27a might reverse multidrug resistance of esophageal squamous cell carcinoma. *Dig Dis Sci* 2010; 55: 2545-2551.
- [15] Zhao XH, Yang L and Hu JG. Down-regulation of miR-27a might inhibit proliferation and drug resistance of gastric cancer cells. *J Exp Clin Cancer Res* 2011; 30: 55.
- [16] Liu XQ, Zhou ZW and Wang ZQ. The DNA damage response molecule MCPH1 in brain development and beyond. *Acta Biochim Biophys Sin (Shanghai)* 2016; 48: 678-685.
- [17] Tubbs A and Nussenzweig A. Endogenous DNA damage as a source of genomic instability in cancer. *Cell* 2017; 168: 644-656.
- [18] Peng G, Yim EK, Dai H, Jackson AP, van der Burgt I, Pan MR, Hu RZ, Li KY and Lin S. BRIT1/MCPH1 links chromatin remodelling to DNA damage response. *Nat Cell Biol* 2009; 11: 865-872.
- [19] Yang SZ, Lin FT and Lin WC. MCPH1/BRIT1 cooperates with E2F1 in the activation of checkpoint, DNA repair and apoptosis. *EMBO Rep* 2008; 9: 907-915.
- [20] Yu CY, Jerry Teng CL, Hung PS, Cheng CC, Hsu SL, Hwang GY and Tzeng YM. Ovatoiodolide isolated from *Anisomeles indica* induces cell cycle G2/M arrest and apoptosis via a ROS-dependent ATM/ATR signaling pathways. *Eur J Pharmacol* 2018; 819: 16-29.
- [21] Lane SIR, Morgan SL, Wu TY, Collins JK, Merriman JA, Ellnati E, Turner JM and Jones KT. DNA damage induces a kinetochore-based ATM/ATR-independent SAC arrest unique to the first meiotic division in mouse oocytes. *Development* 2017; 144: 3475-3486.
- [22] Xia Y, Xu TT, Wang CB, Li YH, Lin ZF, Zhao MQ and Zhu B. Novel functionalized nanoparticles for tumor-targeting co-delivery of doxorubicin and siRNA to enhance cancer therapy. *Int J Nanomedicine* 2018; 13: 143-159.
- [23] Li RN, Liu B, Li XM, Hou LS, Mu XL, Wang H and Linghu H. DACT1 overexpression in type I ovarian cancer inhibits malignant expansion and cis-platinum resistance by modulating canonical Wnt signalling and autophagy. *Sci Rep* 2017; 7: 9285.
- [24] Vickova R, Sopkova D, Andrejckakova Z, Valocký I, Kádasi A, Harrath AH, Petrilla V and Sirotkin AV. Dietary supplementation of yucca (*Yucca schidigera*) affects ovine ovarian functions. *Theriogenology* 2017; 88: 158-165.
- [25] Wang XD, Yan YP, Yang L, Li M and Zhong XH. Effect of quercetin on the expression of Bcl-2/Bax apoptotic proteins in endometrial cells of lipopolysaccharide-induced-abortion. *J Tradit Chin Med* 2016; 36: 737-742.